

Chapter 58

Analysis of Multi-scale Meteorological Parameter Triggering Seroja Tropical Cyclone and Its Effect on Extreme Rainfall Over Nusa Tenggara Timur



Luthfiyah Jannatunnisa and Trismidianto

Abstract From April 1–6, 2021, a tropical cyclone caused extreme rainfall resulting in flooding in several areas in Nusa Tenggara Timur. This paper explained the analysis of multi-scale meteorological parameters during tropical cyclone Seroja events and their effects on rainfall on the island of NTT. Convective activity and rainfall during tropical cyclones were analyzed using Himawari-8 IR1 data and GSMaP data, respectively. Analysis of atmospheric parameters used ECMWF ERA-5 data, and several indices were used to see their interactions with global atmospheric phenomena. There are four stages of development of the Seroja tropical cyclone, namely disturbance, tropical low, mature, and decay phases, with the peak of cyclone occurrence on April 5, 2021. High convective activity began to be seen in the south of Nusa Tenggara Timur during the disturbance and low tropical phases and spread throughout Nusa Tenggara Timur during the mature stage and began to move further south during the decay phase. Tropical cyclones occur during strong Madden Julian Oscillation transitions between phases 4 and 5, which are triggers for intense convective activity during hurricanes, besides being influenced by low-level solid divergence, contributed by winds from the north and south. This tropical cyclone also causes the weak effect of the Borneo vortex around Kalimantan due to the strong attraction of the mass of water vapor by the tropical cyclone. Tropical cyclones also cause changes in the movement of monsoon winds across the island of Sumatra. Compared to rainfall data, the intensity of rainfall over several areas in Nusa Tenggara Timur began to increase ever since the tropical cyclone peak and continued to rise although the cyclone was slowly decaying. With this result, we hope future, we can anticipate the impact of any tropical storms that arise near Indonesia.

L. Jannatunnisa

Meteorological Study Program, Bandung Institute of Technology, Bandung, Indonesia

Trismidianto (✉)

Research Center for Climate and Atmosphere, National Research and Innovation Agency (BRIN), Bandung, Indonesia

e-mail: trismidianto@brin.go.id

58.1 Introduction

A tropical cyclone (TC) is a synoptic-scale meteorological phenomenon in the form of a large storm and grows on warm sea levels ($> 26.5\text{ }^{\circ}\text{C}$) with convective cloud areas. The wind speed around the center of the TC itself is more than 63 km/h (34 knots). The average TC lives between 3 and 18 days, which weakens when entering cold water areas or land. The average lifespan of a TC from growth to extinction is about seven days but can vary from 1 to 30 days. The terms used to describe TC's also vary globally; for example, in the North Atlantic Ocean, this event is called Hurricane, etc. For Indonesia itself, the naming of TC's varies throughout the world; in Indonesia, alone TC's are named after the names of flowers and fruits so that they are easy to remember by the public.

TC occurs in tropics or subtropics areas in the form of storm winds. It begins with the presence of tropical or low-pressure centers that are intensive over the oceans, thus triggering an intensive process of convection and cloud formation. The study of TC has long been introduced by Fasiq (1913) in a book that contains traces, the beginning and destructive action of TC. Many studies of TC are also carried out separately in various cyclone basins of this Earth. However, based on historical events, generally, TC is formed effectively above the 10° N and 10° S region. Therefore, Indonesia's territory should be free from TC formation, but still, there is some part of Indonesia are adjacent to the formation and trajectory of TC [1]. TC's are among the most deadly and destructive natural disasters in terms of loss of human life and economic destruction [2]. Thus, interest in research on tropical cyclones has increased substantially, especially true regarding the study of intraseasonal and interannual variations in the intensity and occurrence of tropical storms, as associated with such phenomena as the Madden Julian Oscillation (MJO—e.g., Maloney and Hartmann [3]), the Quasi-biennial Oscillation (QBO—e.g., Gray et al. [4]), the El Niño and Southern Oscillation (ENSO), and the Pacific Decadal Oscillation (PDO)/North Atlantic Oscillation (NAO) (e.g., Gray et al. [4]; Chan [5]; O'Brien et al. [6]; Houghton et al. [7]).

On April 1, 2021, TC Seroja began to grow in the waters in Luwu Sea near Nusa Tenggara Timur (NTT). In general, TC occurs at latitudes that are more than 10° , but this TC Seroja is a rare cyclonic phenomenon because it occurs at low latitudes. The previous TC Seroja seed of TC 99S that appeared on April 2, 2021, which began to form in the south of NTT, Indonesia, on April 3, 2021. This TC caused floods and hurricanes in several NTT, Indonesia, and Timor Leste, which brought a powerful rainstorm. Rain and wind hit almost the entire scope of NTT, even to Timor Leste, with moderate, heavy, to extreme intensity. The Savu Sea is turbulent. There are waves as high as 4–6 m in the middle of the sea that produce tidal waves with waves as high as 1–1.5 m on the beach. On land, the TC Seroja wreaks havoc on rain-wind for hours, accompanied by lightning, and wreaks havoc. River overflows, tidal waves, flash floods, even cold lava floods, and landslides on Lembata Island. Fallen trees, houses were washed away, bridges fell by the swift river water, mud floods, and some other impacts occurred almost simultaneously in the early hours

of the morning until the morning of Sunday April 4, 2021. Based on data from the National Disaster Management Agency (BNPB), on April 28, 2021, there were 20 districts and one city hit by the TC Seroja, in which 182 people died. Forty-seven people were missing, 132 people were injured, 84,876 people were displaced, and 3516 units of public and social facilities were damaged.

TC dramatically affects the surrounding weather conditions. Some studies have examined the contribution of TCs to precipitation at the regional scale [8, 9]. Villarini and Denniston [10] showed a higher probability of TC-induced annual maximum rainfall events in Australia during La Niña. Yin et al. [11] pointed out that the number of TC-heavy rain days is higher during El Niño years in eastern China; besides that, the phenomenon of TC's can also be related to local, meso, or other global phenomena [12]. TC's affect not only the trajectory area directly but also affects/affected the surrounding weather conditions. Therefore, TCs affect the weather conditions in the Indonesian territory and can occur outside the appropriate period; the storm monitoring / tropical cyclone around Indonesia is essential to do, so that information anticipates a possible impact on the form of bad weather such as floods and landslides [1]. The TC Seroja is also expected to affect the surrounding weather patterns, but the trigger has not been clearly explained. For this reason, an in-depth study of the occurrence of this TC is needed. Based on this, this paper explained the analysis of multi-scale meteorological parameters during TC Seroja events and their effects on rainfall on the island of NTT.

58.2 Data and Method

There are four stages of the TC life cycle which are also seen in the formation of TC Seroja. The division of the stages of the TC cycle is based on information from BMKG at the link <http://tcwc.bmkg.go.id/siklon/learn/03/id>, while for the time event for the stage, it is categorized based on information on TC Seroja from the link <https://zoom.earth/storms/seroja-2021/#layers=daily> so that it can be concluded in Fig. 58.1a. The four stages are the formation stage, immature stage, mature stage, and weakening stage. During the formation stage, an atmospheric disturbance was observed. If observed by satellite, it can be seen that there is a convective area with Cumulonimbus clouds. In the immature stage, the cyclone eye begins to appear, and the strong convective region forms a circular or almost circular cloudy belt. When the TC reaches the mature stage, the cyclonic circulation and gale-force wind area expand. If viewed through satellite imagery, it can be seen that the cloud conditions are more regular and symmetrical and if the intensity is stronger, cyclone eyes can be observed. During the weakening stage, the warm center of the cyclone begins to dissipate, air pressure increases, and the region with maximum wind speed expands and widens away from the center of the cyclone. This stage can occur quickly if a tropical cyclone passes in an area that is not conducive to growth, such as entering high latitude water areas with cold sea surface temperatures or entering the land. These four stages can be seen in the development of TC Seroja; the formation stage

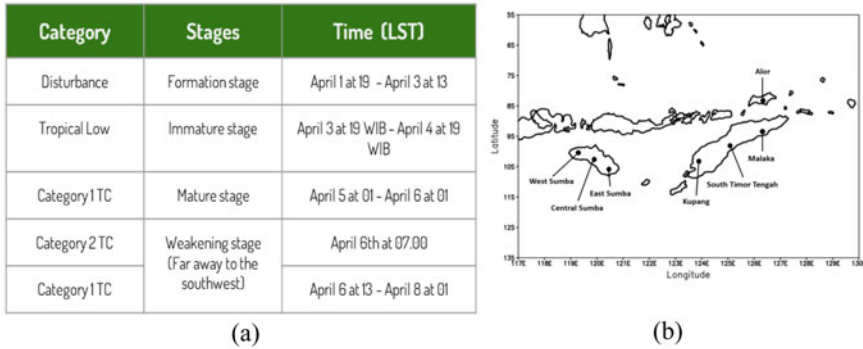


Fig. 58.1 **a** TC Seroja life cycle (source: zoom.earth), **b** NTT and the surrounding area in the study area

occurs in the period of April 1, at 1900 LST (Local Solar Time)–April 3, at 1300 LST with wind speeds of 45 km/h, then on April 3, at 1300 LST–April 4, at 1900 LST there was an increase in rate to 55–65 km/h at immature stage. The peak or ripe stage occurs on April 5, at 0100 WIB–April 6, at 0100 WIB with wind speeds of 85–95 km/h. After that, the impact weakened in the region as the typhoon moved further southwest, despite higher wind speeds. This has an impact in particular on the NTT region. This study examines the effect of tropical cyclones on rainfall in NTT and the surrounding area, as shown in Fig. 58.1b.

In this study, three primary data were used, namely brightness temperature (T_{BB}) from the Himawari-8 satellite, rainfall estimation data from GSMaP, and meteorological parameter data from ECMWF ERA 5. All data is processed using GrADS. The T_{BB} data used in this study was taken from the Himawari-8 satellite operated by the Japan Meteorological Agency (JMA) with a horizontal resolution of $0.05^\circ \times 0.05^\circ$ and temporal resolution of 1 h for infrared (IR) imagery. The Himawari-8 satellite data can be downloaded for free at <http://weather.is.kochiu.ac.jp/sat/GAME>. Analysis of the development of TC Seroja was carried out by visual observation method on the results of plotting Himawari-8 data on IR1 channels by looking at the TBB value. Rainfall estimation data used in this study comes from GSMaP (Global Satellite Mapping of Precipitation) satellite data Near Real-Time (NRT). GSMaP Near Real-Time (GSMaP_NRT) has been implemented since October 2008. Data sets are provided in real-time (about four to five hours after observation) by file transfer protocol (FTP). This GSMaP NRT data from JAXA has been validated and calibrated with both the intelligent and radar data in Japan, with validation results likely to be quite good. GSMaP data can be accessed at <http://sharaku.eorc.jaxa.jp/GSMaP/> (JAXA, 2014). The TC Seroja on the surrounding rainfall is seen by visual observations of rainfall estimates from GSMaP satellite data during the TC Seroja. The movement of the TC Seroja can be analyzed using a hovmoller diagram or cross-section during the occurrence of the TC Seroja.

The meteorological parameter data is obtained from ECMWF ERA5. ERA5 is the fifth generation ECMWF atmospheric reanalysis of the global climate covering January 1950 until present. ERA5 is produced by the Copernicus Climate Change Service (C3S) at ECMWF. ERA5 provides hourly estimates of a large number of atmospheric, land, and oceanic climate variables. The data cover the Earth on a 30 km grid and resolve the atmosphere using 137 levels from the surface up to a height of 80 km. ERA5 includes information about uncertainties for all variables at reduced spatial and temporal resolutions. This data has a time resolution of 6-hourly, a horizontal resolution of $1^\circ \times 1^\circ$ in latitude and longitude in 27 pressure level that include 1000, 975, 950, 925, 900, 875, 850, 825, 800, 775, 750, 700, 650, 600, 550, 500, 450, 400, 350, 300, 250, 225, 200, 175, 150, 125 and 100 hPa. The environmental parameters used in this study are the wind, relative Humidity, temperature, specific Humidity, divergence, vertical velocity, vorticity, and geopotential height. These data can be downloaded at <https://cds.climate.copernicus.eu/#!/search?text=ERA5&type=dataset>. Meteorological conditions analysis is also carried out with the spatial analysis of ECMWF ERA5 data combined with other data.

To analysis the condition of ENSO and IOD, we use the ENSO index and IOD index. The ENSO index is measured from the SST anomaly, Nino 3.4, and the Tahiti-Darwin IOS, which is defined as the difference in Sea Level Pressure (SLP) anomaly in the East Pacific, Tahiti (17.6° S, 149.6° W) with SLP in the West Pacific, Darwin (12.4° S, 130° E). Nino 3.4 covers part of the Nino 3 and Nino 4 areas, which are located at 120° W– 170° W and 5° S– 5° N. Monthly ENSO index data are obtained from the website <http://www.cpc.ncep.noaa.gov>. The IOD index is determined from the difference in the western equatorial Indian Ocean SST anomaly (50° E– 70° E/ 10° S– 10° N) with the Indian Ocean SST anomaly off the coast of Sumatra (90° E– 110° E/ 10° S–Equator). Monthly IOD Index data are obtained from the BOM (Australian Bureau of Meteorology) website <http://www.bom.gov.au/climate/iod/>. To analyze of MJO phase, we use the MJO index from the Real-time Multivariate MJO series 1 (RMM1) and 2 (RMM2). The RMM1 and RMM2 together provide information on the state of the MJO in all parts of the tropics, and have been demonstrated by Wheller and Hendon [13] to be applicable in all seasons. As long as MJO activity was identified, RMM1 led RMM2 around the fourth cycle, indicating MJO propagation eastward along the equator. MJO index data was obtained from the CPC (Climate Prediction Center) website, NOAA (<https://www.cpc.ncep.noaa.gov/products/precip/CWlink/MJO/>). Analysis of monsoon condition in this study based on the data from this link <http://apdrc.soest.hawaii.edu/projects/monsoon/seasonal-monidx.html>.

58.3 Result and Discussion

58.3.1 T_{BB} and Precipitation Analysis

The evolution of the TC Seroja can be analyzed using T_{BB} from the Himawari-8 satellite data shown in Fig. 58.2. TC Seroja seeds began to appear at night at 1900 LST on April 1, 2021, which is the beginning of the formation stage of TC Seroja. This stage lasts long enough until April 3, 2021, at 1300 LST. At this stage, an atmospheric disturbance has been seen. From the night of April 1, 2021, until the early morning of April 2, 2021, it has been seen that there are convective areas with small convective clouds in the land area above the city of Kupang and around the Timor Sea. These small convective clouds continued to grow large scale until noon on April 3, 2021. At this stage, there was no visible center of circulation, but sometimes a spiral-shaped end of the cloud belt can be seen, as shown in figures f1–h1, from morning to noon on April 3, 2021.

On the evening of 1900 LST on April 3, 2021, the immature stage began to occur. At this stage, it is clear that convective solid areas form a protective belt or are almost round and spread in several regions around the TC area. The eye of the cyclone at the circulation center has also begun to be seen and formed since the morning at 0700 LST on April 4, 2021, as shown in figures d2–h2. The mature stage of TC began to occur in the early hours of April 5, 2021, at 0100 LST. At this stage, the cyclonic circulation was seen expanding, and the cloud conditions were more regular, and the intensity was more vigorous. The cyclone eye began to look strong on April 5, 2021,

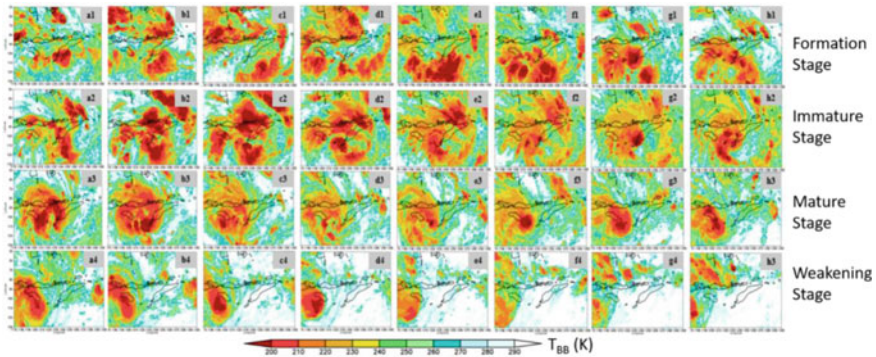


Fig. 58.2 Horizontal distribution of brightness (T_{BB}) temperature on 1–8 April, 2021 during TC Seroja. Figure a1–h1 shows the formation stage where a1–b1 on April 1 at 1900 LST and April 2 at 0100 LST, c1–e1 on April 2 at 0700, 1300, 1900 LST, and figure f1–h1 on April 3 at 0100, 0700, 1300 LST. Figure a2–h2 shows the immature stage where a2 on April 3 at 1900 LST, b2–h2 on April 4 at 0100, 0400, 0700, 1000, 1300, 1600, 1900 LST. Figure a3–h3 shows the mature stage, a3–h3 April 5 at 0100, 0400, 0700, 1000, 1300, 1600, 1900, 2200 LST. Figure a4–h4 shows the weakening stage where the cyclone moving southwest, a4–h4 April 6 at 0100, 0400, 0700, 1000, 1300, 1600, 1900, 2200 LST. T_{BB} unit is Kelvin (K)

over the island of Rote Ndao. TC Seroja started to weaken in the morning at 0700 LST on April 6, 2021. The cyclone’s eyes began to shrink, and convective clouds started to decrease in intensity, and the spiral cloud belt began to disappear. At this stage of attenuation, the movement of cyclones to the surrounding area, the south coast of the island of NTT, and its surroundings are also visible.

Figure 58.3 shows an influence of TC Seroja on rainfall, and the pattern follows the TBB pattern in Fig. 58.2. From Fig. 58.3, we can see that at the formation stage, namely from 1 to 3 April 2021, there has been moderate-intensity rain over Kupang and several areas around it. East Sea. Then at the immature stage since the night of April 3, 2021, until the evening of April 4, 2021, there was rain with moderate to a heavy intensity which had spread over NTT and the surrounding area, especially in the area around the eye of the storm, then at the ripe stage since the early hours of the morning, April 5, 2021, it was already seen that the intensity of hefty rainfall occurred across almost all areas in NTT and the surrounding area. During the weakening stage, the power of precipitation began to decrease significantly, and TC Seroja began to leave NTT and the surrounding area towards Australia.

Figure 58.4a shows time series rainfall in several affected areas from TC Seroja. From the graph, we can see that in Rote Ndao Regency, it rained with very heavy intensity from the formation stage to the immature stage, besides that at the immature stage there was also hefty rain in East Sumba, West Sumba, Sabu Raijua. During the mature stage of TC Seroja, it was seen that there was very heavy rainfall intensity in Central Sumba, East Sumba, and West Sumba. Rainfall intensity decreased significantly in these areas when the TC started to weaken. Reinforced by daily rainfall observations from several BMKG observation stations in NTT as shown in Fig. 58.4b, we can see that in Kupang, Rote Ndao, and East Flores, rainfall with extreme intensity

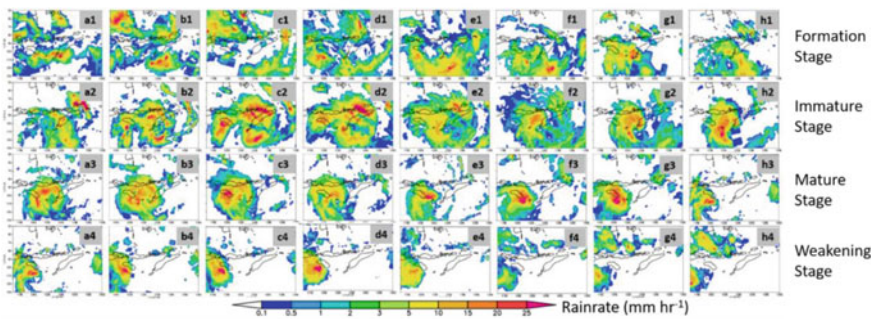


Fig. 58.3 Horizontal distribution of rainfall estimation from GSMaP data on 1–8 April, 2021 during TC Seroja. Figure a1–h1 shows the formation stage where a1–b1 on April 1, at 1900 LST and April 2, at 0100 LST, c1–e1 on April 2, at 0700, 1300, 1900 LST, and figure f1–h1 on April 3, at 0100, 0700, 1300 LST. Figure a2–h2 shows the immature stage where a2 on April 3 at 1900 LST, b2–h2 on April 4 at 0100, 0400, 0700, 1000, 1300, 1600, 1900 LST. Figure a3–h3 shows the mature stage, a3–h3 April 5 at 0100, 0400, 0700, 1000, 1300, 1600, 1900, 2200 LST. Figure a4–h4 shows the weakening stage where the cyclone was moving southwest, a4–h4 April 6, at 0100, 0400, 0700, 1000, 1300, 1600, 1900, 2200 LST. Rainrate unit is mm h^{-1}

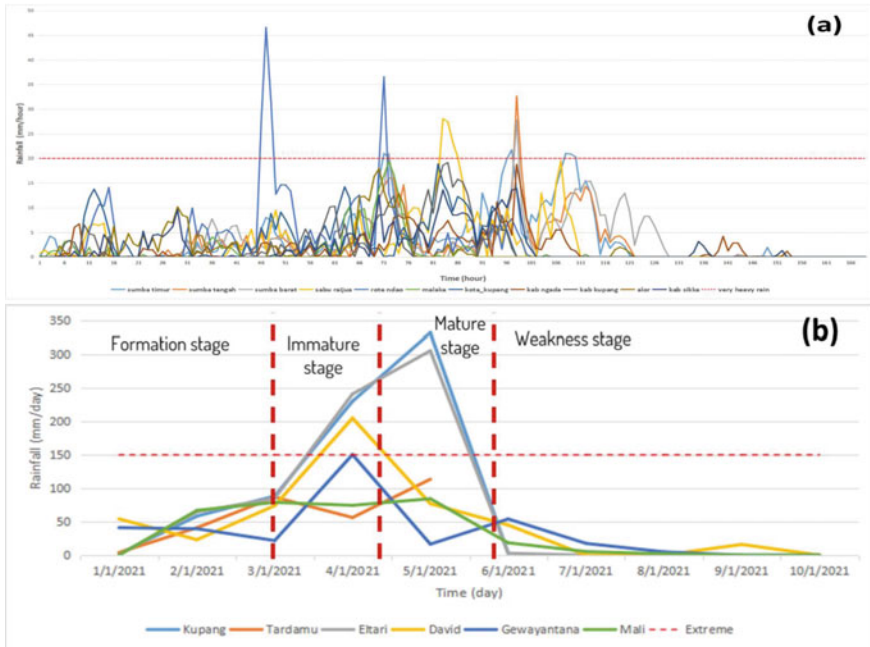


Fig. 58.4 a Hourly rainfall time series from GSMaP data, and b daily rainfall observation from BMKG data, during TC Seroja occurred

is even more during the period of the Seroja tropical cyclone, namely 4–5 April 2021. And after the TC weakened, the intensity of rainfall began to decrease drastically.

One way to show the movement of a rainfall cloud or TC is to create and analyze a hovmoller diagram, as shown in Fig. 58.5a. In this study, a hovmoller diagram was carried out by averaging the longitude of the area of the TC Seroja from 117° to 130°

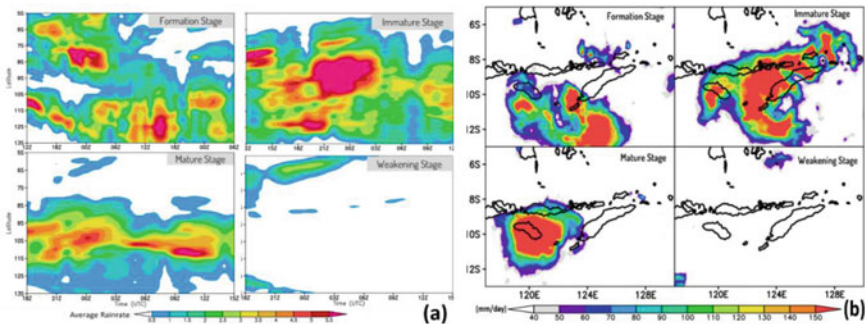


Fig. 58.5 a Time–latitude cross-section in longitude averaged between 117° and 130° for rainfall and b rainfall accumulation in every stage during TC Seroja occurred

E. The hovmoller diagramming is carried out evenly because the cyclone movement is estimated from top to bottom with time changes. The formation stage of the TC Seroja was triggered by the incorporating of several rainfall clouds from the land over NTT at a latitude of around 7° – 8° S with the presence of rainfall clouds from the waters of the Timor Sea around latitude 11° – 13° S with high rainfall intensity. The rainfall cloud combination triggers the occurrence of the TC Seroja with extreme rainfall intensity at its center over NTT during the immature and mature stages. This high rainfall occurs after the peak of the TC Seroja. During the Weakening stage of the TC, the rainfall intensity decreases significantly. Rainfall accumulation for eight days (April 1–8, 2021) using GSMaP satellite data was conducted to see which areas had the most influence during the occurrence of the TC Seroja. Figure 58.5b shows that high rainfall intensities during the formation stage were seen over the Rote Ndao islands and the Timor Sea. And the power of hefty rainfall extends in several areas in NTT; during the mature stage, the power of precipitation is very high. The power of precipitation over NTT has decreased drastically, and there is even no more rainfall over NTT.

58.3.2 Atmospheric Condition Analysis

Based on the streamline plot in Fig. 58.6, we can see that the direction of the wind flows at the time of the TC Seroja incident. Seroja tropical cyclone is seen causing the gathering of air masses originating from the South China Sea, Indian Ocean, and Southern Pacific Ocean. This condition shows that the energy of tropical cyclone Seroja is quite large, even after moving away from Indonesia, the Fujiwhara effect occurs, where tropical cyclones Seroja and Odette rotate cyclonically with each other, according to the definition of the National Weather Service is a binary interaction in which tropical cyclones are within a certain distance (300–750 nautical miles depending on the size of the tropical cyclone) each other begin to rotate around the exact midpoint. Finally, tropical cyclone Seroja was able to survive and continue to move to mainland Australia. During the occurrence of TC Seroja, there was also a Borneo vortex, but it did not last long, and there was no significant effect of the Borneo vortex on the surrounding rainfall; this was due to the weakening of the Borneo vortex from TC Seroja. From the streamline, we also seen that there is the power of TC Seroja to attract the wind in the Indian Ocean so that it moves across the oceanic islands towards the center of the occurrence of TC.

The divergence parameter at the 850 hPa level indicates the level of diffused air, positive values indicate the presence of diffuse/divergent perspective, and harmful for concentrated/convergent air. At this level, we can see from the tropical disturbance stage (Figures a and b) that the air is concentrated and increasingly dark blue / increasingly hostile until the Seroja cyclone moves away to the southwest. This convergent condition affects the occurrence of an updraft. Figure 58.6 also shows the atmospheric parameter of divergence at an altitude of 200 hPa, where figures a and b are dated April 3, at 0700 and 1300 LST. Figures c and d are dated April 4, at

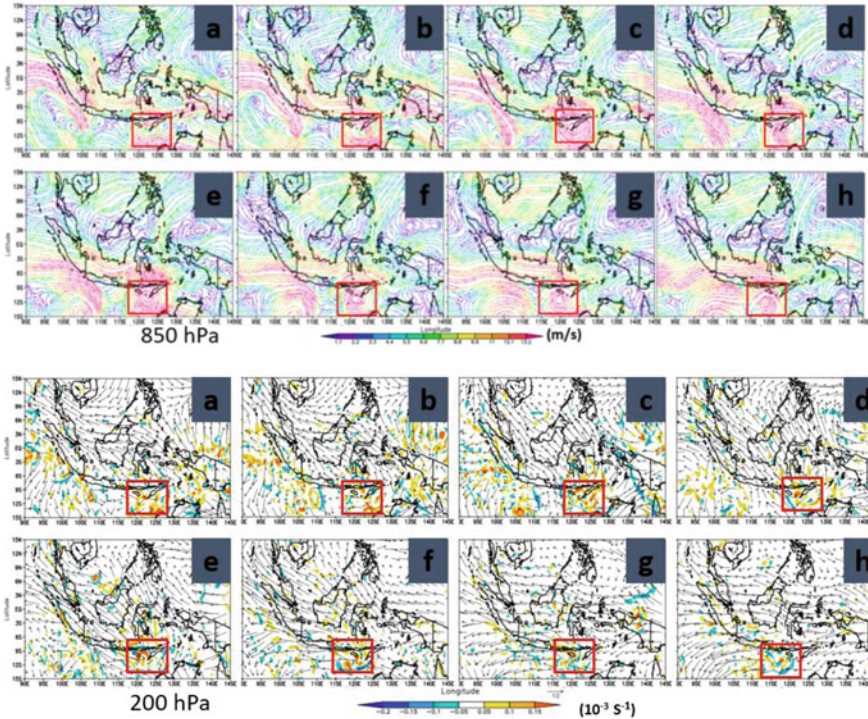


Fig. 58.6 The streamline colored with wind speed and divergence (shaded) at an altitude of 850 hPa and 200 hPa from the reanalyzed ERA5. Figure **a** and **b** on April 3, at 0700 and 1300 LST. Figure **c** and **d** April 4, at 0700 and 1900 LST. Figure **e** and **f** on April 5, at 0700 and 1900 LST. Figure **g** and **h** April 6, at 0700 and 1900 LST

0700 and 1900 LST. Images **e** and **f** on April 5, at 0700 and 1900 LST. Images **g** and **h** April 6, at 0700 and 1900 LST. Then at an altitude of 200 hPa, the air distribution in all directions gets stronger until TC Seroja moves away to the southwest, which means that the intensity of updraft events decreases.

Figure 58.7 shows the composite atmospheric parameters between temperature (shaded) and geopotential (contour) at an altitude of 500 hPa, where Figures **a** and **b** show conditions on April 3, at 0700 and 1300 LST. Figures **c** and **d** show conditions on April 4, at 0700 and 1900 LST. Figures **e** and **f** show conditions on April 5, at 0700 and 1900 LST. Figures **g** and **h** show conditions on April 6, at 0700 and 1900 LST. Low geopotential areas are named with the notation LOW or L, which is indicated by the arrangement of closed geopotential contours getting smaller and smaller. The area with a low geopotential height coincides with an area of low pressure which indicates the presence of a tropical cyclone, for temperature, we can see that the conditions in which tropical cyclones have a higher temperature than other environments. Figure 58.7 also shows the relative humidity conditions during the TC Seroja incident. Relative humidity shows the ratio between water vapor pressure (e)

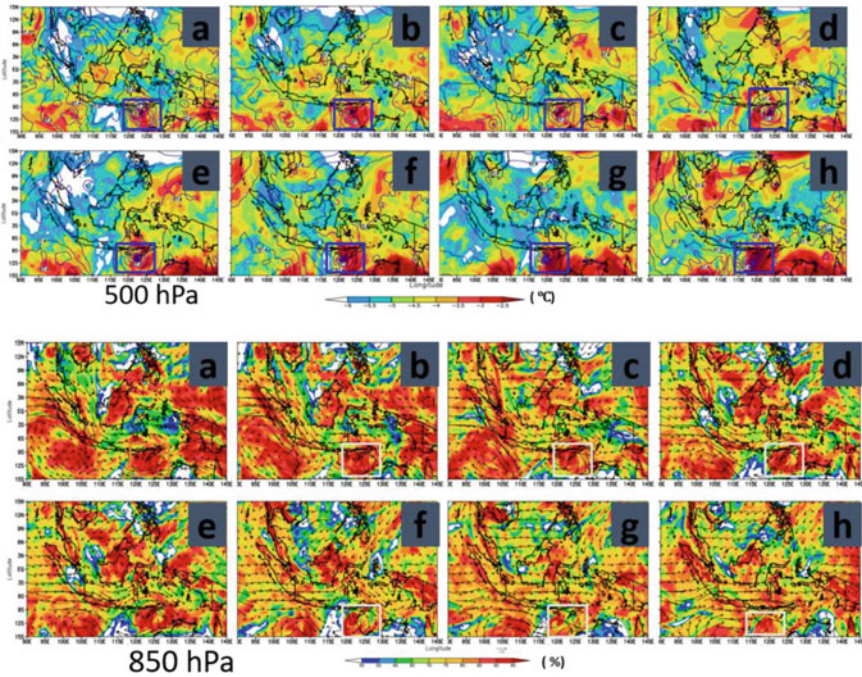


Fig. 58.7 The atmospheric composite parameter between temperature (shaded) and geopotential (contour) at an altitude of 500 hPa (Figure above), and relative humidity at a height of 850 hPa (Figure below) where **a** and **b** on April 3, at 0700 and 1300 LST. Figures **c** and **d** show condition on April 4, at 0700 and 1900 LST. Images **e** and **f** on April 5, at 0700 and 1900 LST. Images **g** and **h** April 6, at 0700 and 1900 LST

and saturated water vapor pressure (ice) at the same temperature. We can see that the RH during the TC Seroja shows more than 95%, which means the air is saturated or humid.

Figure 58.8 shows that at the stage of cyclone formation, especially on April 2, at 0100 and 0700 LST, it is seen that there is a strong convergence at an altitude of around 950–800 hPa and a substantial divergence at the 300–100 hPa layer. Then when the immature stage was seen on April 3, at 1900 LST–April 4, at 0700 LST, there was an expansion of the convergence strengthening area and on April 4, at 1100–1600 LST, there was also a strong convergence in the 500–350 hPa layer. And in the mature stage, strong convergence occurs at the level of 1000–950 hPa, and there is an expansion of the divergence area at the level of 250–100 hPa. By the time the TC has started to weaken where the cyclone is beginning to move away, it seems that there are no events, either convergent or divergent. For the vertical velocity contour, we can see that from the cyclone formation stage until it matures, the value is negative, which means an updraft occurs, where the moist air mass will rise, and when the cyclone moves away to the southwest, the area that is not affected by the

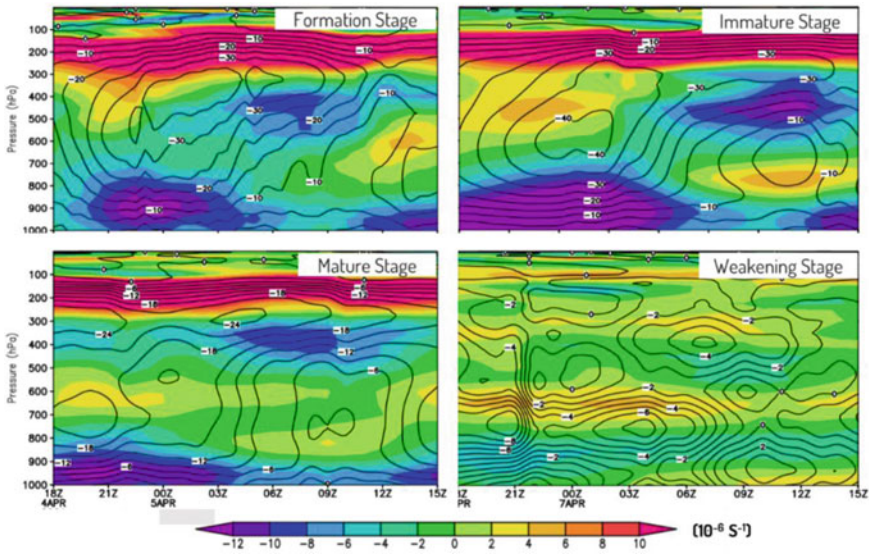


Fig. 58.8 Pressure–time cross-section for composite between the divergence (shaded, 10^{-6} S^{-1}) and the vertical velocity (contour, $10^{-2} \text{ Pa s}^{-1}$) in every stage during TC Seroja occurred. By averaging the values of divergence and vertical velocity for latitude and longitude in the area of TC Seroja (15° and 5° S) and 117° – 130° E)

tropical cyclone shows an increasing value towards positive where updraft activity decreases.

58.3.3 Interannual and Interseasonal Variability Analysis

In general, the causes of rainfall in Indonesia are influenced by several phenomena, including ENSO and IOD as the coupled ocean–atmosphere modes in the tropical Indo-Pacific region, which have a significant impact on the rain over the maritime continent [14, 15]. ENSO is a leading mode of tropical climate variability at inter-annual timescales and is characterized by sea surface temperature (SST) and surface pressure anomalies across the Pacific Ocean. Its positive “El Niño” phase occurs when SSTs are warm in the eastern tropical Pacific Ocean, contrasted by its negative “La Niña” phase when they are cool. The IOD is another coupled ocean–atmosphere mode [16], with a positive (negative) phase characterized by warm (cool) SSTs over the western Indian Ocean and cool (warm) SSTs in the eastern Indian Ocean. The two phenomena activities often co-occur, resulting in a decrease in the amount of rainfall (drought) and increased rainfall (floods) in some parts of Indonesia. Another phenomenon that also dramatically affects rainfall in Indonesia is the Madden–Julian Oscillation (MJO) as the significant intraseasonal (30–60 days) variability in the

tropics, characterized by the eastward propagation of cloud clusters and precipitation from the Indian Ocean to the western Pacific Ocean [17]. The influence of the MJO on Indonesian precipitation variability has been generally discussed by several authors [18–20].

Figure 58.9a shows that the IOD Index was positive in April when the Seroja TC occurred; this indicates that the west coast of Sumatra has high pressure, while the east coast of the African continent has low pressure so that airflow from the west of Sumatra will go east of Africa which results in cloud formation. Convective clouds over Africa and produce above-normal rainfall. On the other hand, in the western region of Sumatra, there is a drought after the mass of water vapor fails to reduce it as rain. The existence of the high-pressure area of the west coast of Sumatra also supports the movement of wind or water vapor masses to regions of low pressure, including towards TC Seroja. This strengthens Fig. 58.6, where there is wind movement from the west coast of Sumatra across the island of Sumatra to the TC Seroja area. Figure 58.9b shows that the ENSO Index in April 2021 was in a weak La Nina condition where the easterly winds along the equator became stronger than usual and generally impacted the form of increased rainfall in the western equatorial Pacific, including Indonesia. La Nina conditions also trigger the growth of convective clouds in Indonesia, especially in central Indonesia; this condition is possible one of the triggers for the development of convective clouds around the area where TC Seroja occurs during the formation stage and also makes the life cycle of TC also long.

Figure 58.10 shows the sea surface temperature (SST) on March 29–April 4, 2021 around the NTT area. The SST value is in the range of 29–30 °C, where this condition makes the NTT region have lower pressure than other regions and this high SST is a contributor to high rainfall because it supports the growth of a lot of convective clouds that trigger the occurrence of TC Seroja.

According to Khromov [21], monsoon areas are areas where the dominant wind direction reverses at least 120° between January and July. January is the winter maximum in the northern hemisphere with the lowest average temperature in the

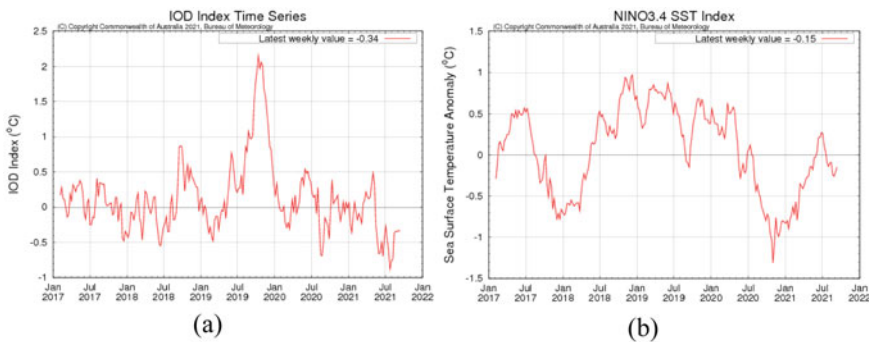


Fig. 58.9 a IOD index and b NINO 3.4 Index from the Bureau of Meteorology (BOM)

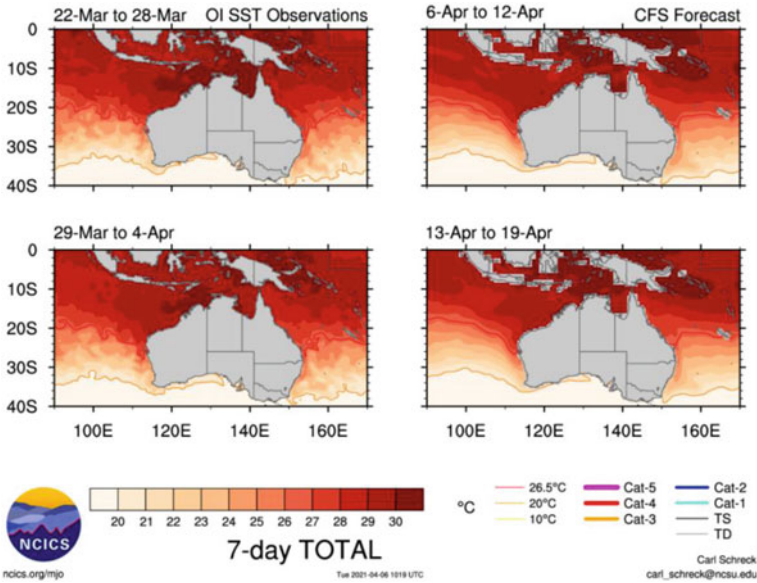


Fig. 58.10 Sea surface temperature during TC Seroja occurred

northern hemisphere, and July is the summer maximum with the highest average temperature in the northern hemisphere. Ramage [22] defines of monsoon by adding wind strength criteria and identifying areas including Africa, Asia, and Australia as areas that meet both the reverse wind criteria and the monsoon rain criteria. Figure 58.11 shows the WPMI value (Asian monsoon index) during April 2021 getting stronger until May 2021, and for the Australian monsoon, on the contrary, it is weakening. *This* shows the impact that when the Asian monsoon winds flow, Indonesia will experience the rainy season in April, which is also the trigger for many convective clouds before the Seroja TC.

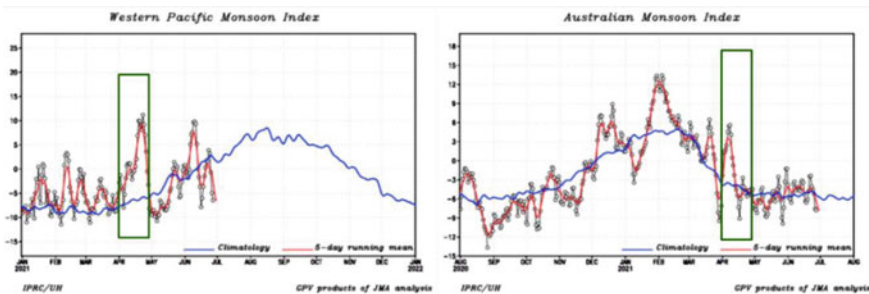


Fig. 58.11 Western Pacific Monsoon index (left) and Australian Monsoon index (right) from Japan Meteorology Agency (JMA)

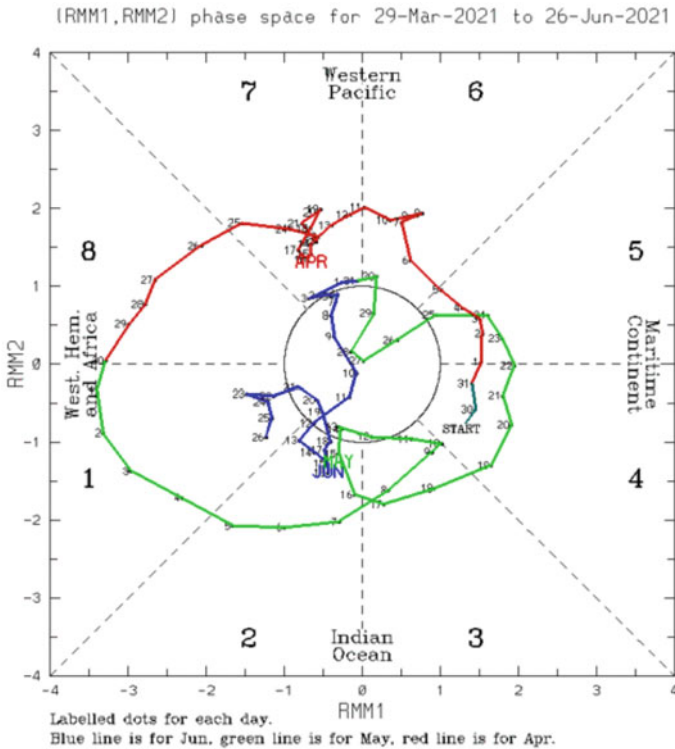


Fig. 58.12 MJO index during TC Seroja occurred

The MJO index on April 1–5, 2021, shows that the condition of the MJO is entering phases 4 and 5 as shown in Fig. 58.12. The index values for Phase 4 and 5, also show values above 1, which means that there is a strong MJO in the Indonesian maritime continent. So with the active MJO, it increases the possibility of many convective clouds in Indonesia, which is believed also to trigger the development of convective clouds into TC Seroja.

58.4 Conclusions

TC Seroja seeds began to appear at night at 1900 LST on April 1, 2021, which is the beginning of the formation stage of TC Seroja. This stage lasts long enough until April 3, 2021, at 1300 LST. On the evening of 1900 LST on April 3, 2021, the immature stage began to occur. At this stage, it is clear that strong convective areas form a protective belt or are almost round and spread in several regions around the TC area. The mature stage of TC began to occur in the early hours of April 5, 2021, at 0100 LST. At this stage, the cyclonic circulation was seen expanding, and the cloud

conditions were more regular, and the intensity was more vigorous. TC Seroja began to weaken in the morning at 0700 LST on April 6, 2021. The effect of the Seroja tropical cyclone on rainfall is seen when the cyclone seeds start to form, there is an increase in rainfall in some areas, at the peak of the cyclone, extreme rain occurs in Kupang City, Rote Ndao Regency, East Flores Regency after the cyclone moved away, rain fell still drastically in the NTT area. High convective activity began to be seen in the south of NTT during the disturbance and low tropical phases and spread throughout NTT during the mature stage, and began to move further south during the decay phase. The streamlined pattern shows that the Seroja cyclone causes air masses to gather from the South China Sea, Indian Ocean, and South Pacific Ocean. The divergence at the 200 hPa layer strengthens, and a diffuse air mass is seen. Geopotential contours can be used to show the location of the tropical cyclone, and the temperature is higher than in other environments. This tropical cyclone also causes the weak effect of the Borneo vortex around Kalimantan due to the strong attraction of the mass of water vapor by the tropical cyclone. TC also causes changes in the movement of monsoon winds across the island of Sumatra. TC occurs during strong MJO transitions between phases 4 and 5, which are one of the triggers for strong convective activity during cyclones, besides being influenced by strong low-level divergence, contributed by winds from the north and south. During TC Seroja, ENSO is in a weak La Nina condition, and increased Asian monsoon activity causes the strengthening of convective activity over Nusa Tenggara Timur.

Acknowledgements Thank you so much for the three sources of data, which we can get for free, and the data is beneficial to this research. This research uses data from ECMWF ERA-Interim (<http://www.ecmwf.int/>), Himawari-8 satellite (<http://weather.is.kochi.ac.jp/sat/GAME>) and GSMaP satellite (<http://sharaku.eorc.jaxa.jp/GSMaP/>).

References

1. Haryani, N.S., Any, Z.: *Dinamika Siklon Tropis di Asia Tenggara Menggunakan Data Penginderaan Jauh*. Pusbangja LAPAN, 324 (2012)
2. Bengtsson, L., Bozdet, M., Esch, M.: Will green-house gas-induced warming over the next 50 years lead to higher frequency and greater intensity of hurricanes? *Tellus* **48A**, 57–73 (1996)
3. Maloney, E.D., Hartmann, D.L.: The Madden-Julian Oscillation, barotropic dynamics, and North Pacific tropical cyclone formation. Part I: Observations. *J. Atmos. Sci.* **58**, 2545–2557 (2001)
4. Gray, W.M.: Atlantic season hurricane frequency. Part 1: El Nino and 30 mb Quasi Biennial Oscillation influences. *Mon. Wea. Rev.* **112**, 1649–1668 (1984)
5. Chan, J.C.L.: Tropical cyclone activity in the Northwest Pacific in relation to the El Nino/Southern Oscillation phenomenon. *Mon. Wea. Rev.* **113**, 599–606 (1985)
6. O'Brien, J.J., Richards, T.S., Davis, A.C.: The effect of El Nino on U.S. landfalling hurricanes. *Bull. Amer. Meteor. Soc.* **77**, 773–774 (1996)
7. Houghton, J.T., et al. (eds.): *Climate Change 2001: The Scientific Basis*, 857pp. Cambridge University Press, Cambridge, UK (2001)

8. Chen, F., Fu, Y.: Contribution of tropical cyclone rainfall at categories to total precipitation over the western North Pacific from 1998 to 2007. *Sci. China Earth Sci.* **58**, 2015–2025 (2015). <https://doi.org/10.1007/s11430-015-5103-9>
9. Ng, B., Walsh, K., Lavender, S.: The contribution of tropical cyclones to rainfall in northwest Australia. *Int. J. Climatol.* **35**, 2689–2697 (2015). <https://doi.org/10.1002/joc.4148>
10. Villarini, G., Denniston, R.F.: Contribution of tropical cyclones to extreme rainfall in Australia. *Int. J. Climatol.* **36**, 1019–1025 (2016). <https://doi.org/10.1002/joc.4393>
11. Yin, Y., Gemmer, M., Luo, Y., Wang, Y.: Tropical cyclones and heavy rainfall in Fujian Province, China. *Quat. Int.* **226**, 122–128 (2010). <https://doi.org/10.1016/j.quaint.2010.03.015>
12. Curtis, S., Adler, R.F.: Evolution of El Nino precipitation relationships from satellite and gauges. *J. Geoph. Res.* **108** (2003)
13. Wheeler, M.C., Hendon, H.H.: An all-season real-time multivariate MJO index: development of an index for monitoring and prediction. *Mon. Weather Rev.* **132**, 1917–1932 (2004). [https://doi.org/10.1175/1520-0493\(2004\)132%3c1917:AARMMI%3e2.0.CO;2](https://doi.org/10.1175/1520-0493(2004)132%3c1917:AARMMI%3e2.0.CO;2)
14. Aldrian, E., Susanto, D.: Identification of three dominant rainfall regions within Indonesia and their relationship to sea surface temperature. *Int. J. Climatol.* **23**, 1435–1452 (2003)
15. Nur'utami, M.N., Hidayat, R.: Influences of IOD and ENSO to Indonesian rainfall variability: role of atmosphere-ocean interaction in the Indo-Pacific sector. *Procedia Environ. Sci.* **33**, 196–203 (2016). <https://doi.org/10.1016/j.proenv.2016.03.070>
16. Saji, N.H., Goswami, B.N., Vinayachandran, P.N., Yamagata, T.: A dipole mode in the tropical Indian Ocean. *Nature* **401**(6751), 360–363 (1999)
17. Madden, R.A., Julian, P.R.: Detection of a 40–50 day oscillation in the zonal wind in the tropical Pacific. *J. Atmos. Sci.* **28**, 702–708 (1971). [https://doi.org/10.1175/1520-0469\(1971\)028%3c0702:DOADOI%3e2.0.CO;2](https://doi.org/10.1175/1520-0469(1971)028%3c0702:DOADOI%3e2.0.CO;2)
18. Jones, C., Waliser, D.E., Lau, K.M., Stern, W.: Global occurrences of extreme precipitation and the Madden-Julian oscillation: observations and predictability. *J. Clim.* **17**, 4575–4589 (2004). <https://doi.org/10.1175/3238.1>
19. Hidayat, R., Kizu, S.: Influence of the Madden-Julian oscillation on Indonesian rainfall variability in austral summer. *Int. J. Climatol.* **30**, 1816–1825 (2010). <https://doi.org/10.1002/joc.2005>
20. Xavier, P., Rahmat, R., Cheong, W.K., Wallace, E.: Influence of Madden-Julian oscillation on Southeast Asia rainfall extremes: observations and predictability. *Geophys. Res. Lett.* **41**, 4406–4412 (2014). <https://doi.org/10.1002/2014GL060241>
21. Khromov, S.P.: Die geographische Verbreitung der Monsune. *Petermanns Geographische Mittheilung* **101**, 234–237 (1957)
22. Ramage, C.S.: Role of a tropical “Maritime Continent” in the atmospheric circulation. *Mon. Weather Rev.* **96**, 365–369 (1968)